

# Infrared Study of the Folding Mechanism of a Helical Hairpin: Porcine PYY<sup>†</sup>

Matthias M. Waegelé and Feng Gai\*

*Department of Chemistry, University of Pennsylvania, Philadelphia, Pennsylvania 19104*

*Received May 26, 2010; Revised Manuscript Received July 14, 2010*

**ABSTRACT:** The helical hairpin motif plays a key role as a receptor site in DNA binding and protein–protein interactions. Thus, various helical hairpins have recently been developed to assess the factors that control the DNA and/or protein binding affinities of this structural motif and to form synthetic templates for protein and drug design. In addition, several lines of evidence suggest that rapid acquisition of a helical hairpin structure from the unfolded ensemble may guide the rapid formation of helical proteins. Despite its importance as a crucial structural element in protein folding and binding, the folding mechanism of the helical hairpin motif has not been thoroughly studied. Herein, we investigate the structural determinants of the folding kinetics of a naturally occurring helical hairpin (porcine PYY) that is free of disulfide bonds and metal ion-induced cross-links using an infrared temperature-jump technique. It is found that mutations in the turn region predominantly increase the barrier of folding irrespective of the temperature, whereas the effect of mutations that perturb the hydrophobic interactions between the two helices is temperature-dependent. At low temperatures, deletion of hydrophobic side chains is found to predominantly affect the unfolding rate, while the opposite is observed at high temperatures. These results are interpreted in terms of a folding mechanism in which the turn is formed in the transition state and also based on the assumption that cross-strand hydrophobic contacts exist in the thermally unfolded state of PYY.

The  $\alpha$ -helical hairpin, or helix–turn–helix (HTH)<sup>1</sup> motif, can be regarded as a supersecondary structural element of helical proteins. In many cases, the HTH motif is found to play an important functional role. For example, it is the primary recognition element of a large number of DNA-binding proteins (1, 2) and is also involved in protein–protein interactions (2). Therefore, it is not surprising that there has been great interest in designing stable helical hairpins that exhibit high affinity and specificity toward DNA or proteins (3–5). In addition, the HTH motif has been suggested to play an important role in protein folding. Because it encompasses both secondary structural elements and long-range tertiary contacts, a rapidly formed local HTH conformation could serve as a folding nucleus or kernel (6–8), allowing rapid assembly of the entire tertiary structure. For example, Religa et al. (9) have shown that the fast phase in the folding kinetics of Engrailed homeodomain (EnHD) arises from the formation of a folding kernel consisting of helices 2 and 3 of the protein.

Because of the structural and functional roles of the HTH motif, the structural determinants and folding–unfolding thermodynamics of various helical hairpins have been extensively studied in the past few years (5, 10–12). Though these equilibrium studies provided valuable insights into the factors that control the thermal stability of the HTH motif, they revealed little information about how folding and unfolding actually take place. As a result, our current understanding of the folding mechanism of the HTH motif is mainly based on the kinetic study of a cross-linked  $\alpha$ -helical hairpin, Z34C (13), whose termini are covalently connected via a disulfide bond that is introduced to stabilize the folded struc-

ture (3). While Z34C is a useful template for protein and drug design (3), it may not be a good model system for understanding the mechanism of  $\alpha$ -helical hairpin formation as the disulfide constraint artificially limits the accessible conformational space of the unfolded state ensemble.

To provide further insight into the folding mechanism of the HTH motif, herein we study the folding dynamics of a monomeric, naturally occurring helical hairpin (porcine PYY; sequence, YPAKP-EAPGE-DASPE-ELSRV-YASLR-HYLNH-VTRQR-Y-NH<sub>2</sub>) by means of temperature-jump infrared (*T*-jump IR) spectroscopy (14) in conjunction with site-directed mutagenesis (15). As shown (Figure 1), porcine PYY (hereafter termed PYY) is free of disulfide bonds and assumes a structure known as the PP fold in which an N-terminal type II polyproline (PPII) helix folds onto a C-terminal  $\alpha$ -helix to form a stable, well-defined hydrophobic cluster between the interfaces of the two helices (11, 16, 17). To dissect the kinetic roles of the two most important structural elements in the PP fold, i.e., the hydrophobic cluster and the turn, we studied the folding–unfolding kinetics of two sets of PYY mutants. The first set of mutants, A7Y, Y21A, and Y27A, involves residues that contribute to the hydrophobic interactions between the two helices. The second set of mutants, S13A and P14A, targets residues in the turn region of the peptide. Our results support the notion that the turn sequence has a strong influence on the folding rate of hairpin structures (13, 18, 19) and that the turn sequence in wild-type PYY is highly optimized for folding, whereas the kinetic effect of mutations in the hydrophobic cluster is more complicated.

## MATERIALS AND METHODS

**Materials.** All materials were used as received. D<sub>2</sub>O (D, 99.96%) was purchased from Cambridge Isotope Laboratories (Andover, MA). Amino acids for peptide synthesis were obtained from Advanced ChemTech (Louisville, KY).

<sup>†</sup>Supported by the National Institutes of Health (Grants GM-065978 and RR-01348).

\*To whom correspondence should be addressed. E-mail: gai@saş.upenn.edu. Phone: (215) 573-6256. Fax: (215) 573-2112.

Abbreviations: CD, circular dichroism; IR, infrared; *T*-jump, temperature-jump; HTH, helix–turn–helix.

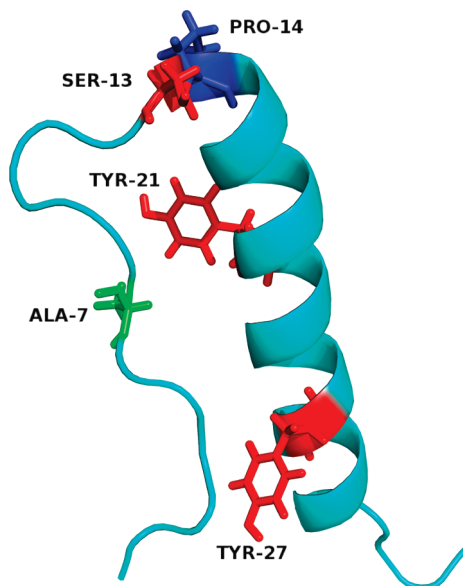


FIGURE 1: NMR structure of porcine PYY (Protein Data Bank entry 2RLK). The side chains of those residues targeted for mutation are shown as sticks.

**Peptide Sample Preparation.** The peptides were synthesized using standard fluorenyl-methoxycarbonyl (Fmoc) chemistry on a PS3 peptide synthesizer from Protein Technologies (Tucson, AZ) and were purified by reversed-phase HPLC (Agilent Technologies, Santa Clara, CA). The mass of each peptide was verified by matrix-assisted laser desorption ionization mass spectrometry (Voyager-DE RP, Applied Biosystems, Foster City, CA). Following purification, the peptide solutions were lyophilized, dissolved in  $D_2O$ , and titrated to  $pH^* 5.2 \pm 0.1$  (pH meter reading) with a solution of sodium hydroxide in  $D_2O$ . Another round of lyophilization in  $D_2O$  ensured complete removal of  $H_2O$ . The peptide samples used in spectroscopic measurements were prepared by dissolving an appropriate amount of lyophilized peptide solid in 20 mM  $D_2O$  2-(*N*-morpholino)ethanesulfonic acid (MES) buffer ( $pH^* 5.2$ ). For circular dichroism (CD) measurements, the peptide concentration was  $\sim 40 \mu M$ , determined optically using the absorbance of tyrosine at 280 nm and an extinction coefficient of  $1492 \text{ cm}^{-1} \text{ M}^{-1}$ . For IR measurements, the peptide concentration was in the range of 1–4 mM.

**CD Measurement and Analysis.** CD data were collected on an Aviv model 410 instrument (Aviv Biomedical, Lakewood, NJ) using a 1 mm cuvette. For thermal unfolding measurements, the CD signal at 222 nm was averaged for 30 s at each temperature. After the highest temperature was reached, the sample was cooled to 25 °C and another full CD spectrum was measured to ensure that unfolding was reversible. The folding–unfolding thermodynamics of PYY and the mutants were determined by globally fitting their CD thermal melting transitions to a two-state model; the details of the global fitting method have been described previously (20). Briefly, the folded and unfolded CD baselines [ $\theta_F(T)$  and  $\theta_U(T)$ , respectively] were assumed to be linear functions of temperature; i.e.,  $\theta_F(T) = m + nT$ , and  $\theta_U(T) = p + qT$ .  $n$  and  $q$  ( $m$  and  $p$ ) were treated as global (local) fitting parameters.

***T*-Jump Relaxation Measurement.** The *T*-jump-induced relaxation kinetics of PYY and mutants were measured by probing the time-dependent absorbance change of the helical amide I' band of the peptide at  $1631 \text{ cm}^{-1}$ . A detailed description of the *T*-jump IR setup can be found elsewhere (21). The only difference

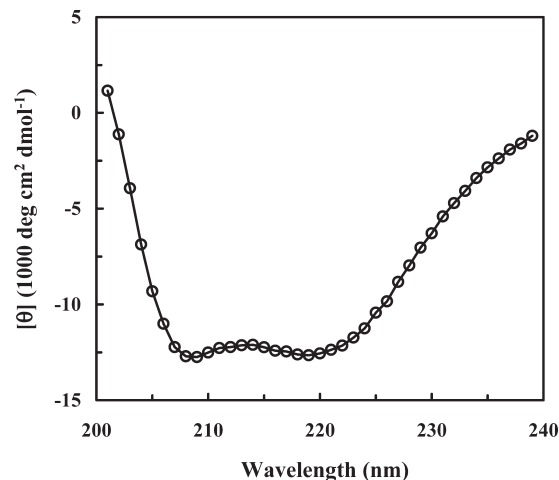


FIGURE 2: Far-UV CD spectrum of PYY at 25 °C.

is that in our study the transient IR signals were probed by a tunable quantum cascade laser (Daylight Solutions, Poway, CA). The *T*-jump-induced relaxation kinetics of the PYY peptides were found to develop in two distinct phases. The fast kinetic phase is unresolvable because of the 20 ns rise time of the IR detector and is attributed to temperature-induced spectral shift and/or imperfect background subtraction. Thus, only the slow phase, which can be described by a single-exponential function, is considered in the following discussion.

## RESULTS AND DISCUSSION

The HTH motif has recently attracted much attention because of its DNA and protein binding properties (3–5, 22) and because of its potential role as a productive (on pathway) intermediate in protein folding (6–8), such as in the case of EnHD (9). Previously, we have shown that the folding mechanism of a cross-linked  $\alpha$ -helical hairpin, Z34C, is similar to that of  $\beta$ -hairpins (13), with turn formation playing a dominant role in the folding kinetics of the hairpin. However, because of the disulfide cross-linker, it is unclear whether the folding mechanism of Z34C is representative of that of unconstrained  $\alpha$ -helical hairpins. Therefore, we extend our study on how  $\alpha$ -helical hairpins fold to porcine PYY (11, 16, 17), a naturally occurring HTH motif free of disulfide bonds.

**Folding Thermodynamics and Kinetics of PYY.** As shown (Figure 2), the far-UV CD spectrum of PYY in phosphate buffer (20 mM,  $pH^* 5.2$ ) at 25 °C exhibits the characteristic double minima of  $\alpha$ -helices, indicating that it is mostly folded at this temperature. To better quantify the folding–unfolding thermodynamics of PYY and the mutants studied here (see below), we globally analyzed their CD melting curves measured at 222 nm using a global fitting method (see Materials and Methods for details). As shown (Figure 3 and Table 1), the thermal melting temperature ( $T_m$ ) of wild-type PYY thus obtained is  $44.0 \pm 1.6$  °C, which is almost identical to that determined by Zerbe and co-workers using NMR spectroscopy (11).

The conformational relaxation kinetics of PYY in response to a *T*-jump were measured using a time-resolved infrared technique (21) with a probing frequency of  $1631 \text{ cm}^{-1}$ , where solvated  $\alpha$ -helical amides exhibit strong absorbance (23–25). As shown (Figure 4), the *T*-jump-induced conformational relaxation of PYY obtained at 32.2 °C, a temperature that is below  $T_m$ , occurs on the microsecond time scale, indicating that it folds very

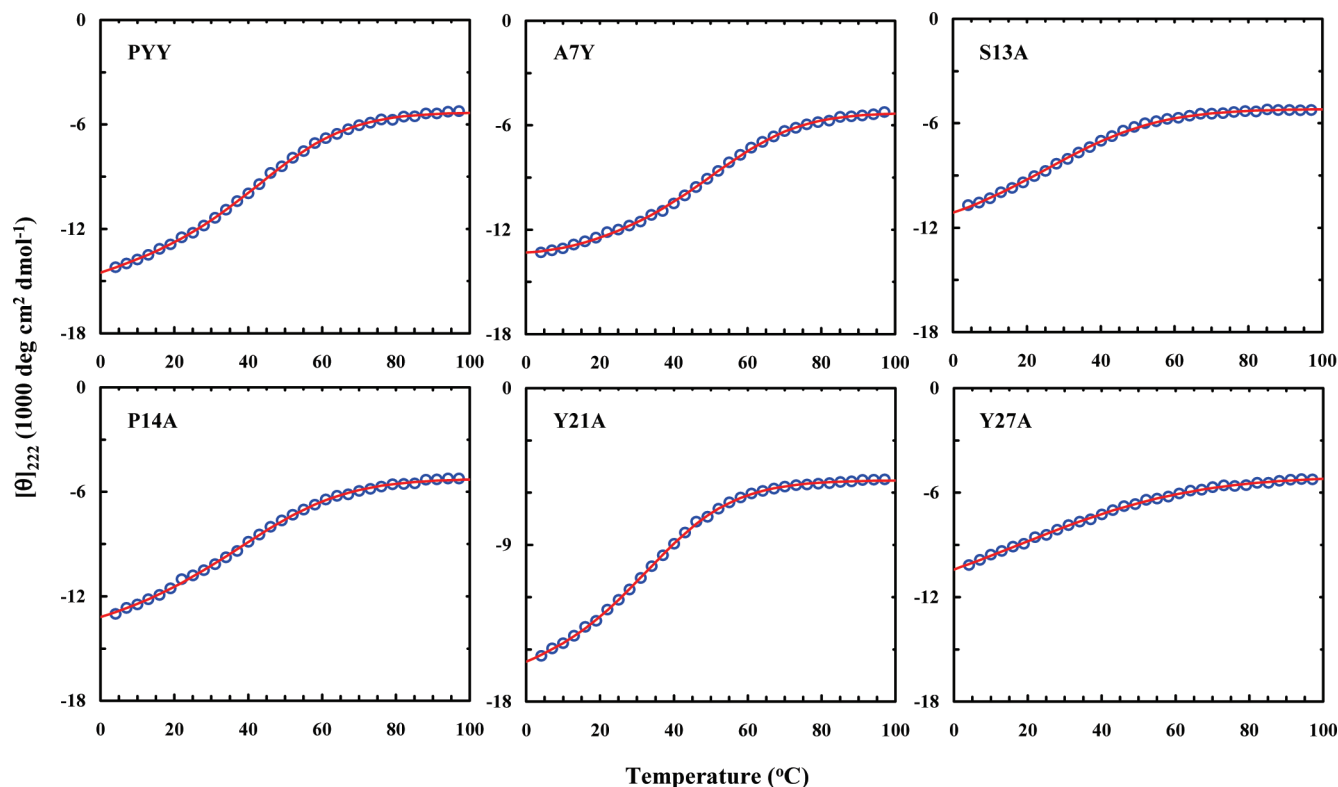


FIGURE 3: Thermal unfolding CD curves of PYY and its mutants, as indicated. Lines are fits to the two-state model described in the text.

Table 1: Unfolding Thermodynamic Parameters of PYY and Its Mutants Obtained from Global Fitting of Their CD Thermal Melting Curves

| peptide | $\Delta H_m^0$<br>(kcal/mol) | $\Delta S_m^0$<br>(cal K <sup>-1</sup> mol <sup>-1</sup> ) | $\Delta C_p$<br>(cal K <sup>-1</sup> mol <sup>-1</sup> ) | $T_m$ (°C) |
|---------|------------------------------|--|--|------------|
| PYY     | 14.5 ± 1.6                   | 45.8 ± 4.8   | 221 ± 25   | 44.0 ± 1.6 |
| A7Y     | 13.5 ± 1.3                   | 41.9 ± 3.9   | 333 ± 47   | 48.7 ± 2.0 |
| S13A    | 5.5 ± 0.7                    | 19.1 ± 2.5   | 221 ± 25   | 13.5 ± 2.0 |
| P14A    | 10.2 ± 0.7                   | 33.1 ± 2.1   | 221 ± 25   | 36.0 ± 1.9 |
| Y21A    | 15.8 ± 0.2                   | 51.4 ± 0.7   | 139 ± 41   | 35.1 ± 0.9 |
| Y27A    | 3.3 ± 0.5                    | 11.8 ± 1.9   | 100 ± 29   | 4.1 ± 2.7  |

rapidly. Indeed, decomposition of the relaxation rate constants into folding and unfolding rate constants based on a two-state analysis (see Materials and Methods for details) shows that the folding time constant of PYY is around 3  $\mu$ s in the temperature range studied (Figure 5). For example, at 30 °C, the folding and unfolding rate constants are  $(2.8 \pm 0.5 \mu\text{s})^{-1}$  and  $(7.1 \pm 1.3 \mu\text{s})^{-1}$ , respectively (Table 2). Interestingly, the  $\alpha$ -helical hairpin Z34C, whose folded structure is stabilized by a disulfide bond that links the N- and C-termini of the peptide, folds with a similar rate (13). Taken together, these results thus corroborate our previous notion that such disulfide bonds stabilize the folded state of the HTH motif by primarily decreasing its unfolding rate (13).

*Effect of the Turn Sequence on the Folding Thermodynamics and Kinetics of PYY.* For  $\beta$ -hairpins, it has been shown that the sequence of the reverse turn plays a critical role in both the stability and folding kinetics of the native fold (18, 19). To explore the role of the turn in PYY folding, we further studied the folding thermodynamics and kinetics of two PYY mutants, S13A and P14A. The choice of these mutations is based on the study by Zerbe and co-workers which showed that both Ser13 and Pro14 are located in the turn region that links the C-terminal  $\alpha$ -helix to the N-terminal polyproline helix and that the Ser13 to Ala

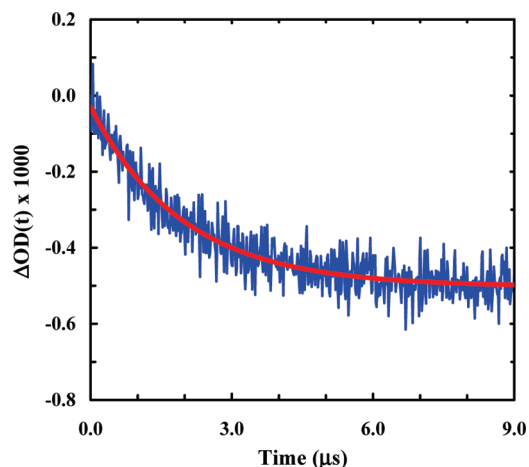


FIGURE 4: Representative relaxation kinetic trace of PYY in response to a  $T$ -jump of 9.2 °C, from 23.0 to 32.2 °C. For the sake of clarity, an unresolved kinetic phase has been subtracted from these data. The smooth line represents the best fit of these data to a single-exponential function with a lifetime of 1.9  $\mu$ s.

mutation is especially disruptive to the native fold of PYY (11). Consistent with their NMR study, our CD results show that both mutations result in a decrease in the thermal stability of the PYY fold and that replacement of Ser13 with Ala is strongly destabilizing (Figure 3 and Table 1). This observation suggests that the native turn sequence in PYY is optimized for folding and is also in agreement with the finding of Hodges and Schepartz (5) that mutations in the turn region destabilize the folded state of a designed derivative of avian pancreatic polypeptide (aPP), whose sequence and fold are similar to those of PYY.

The thermodynamic consequence of a mutation is a direct outcome of its effects on the folding and unfolding rates. For

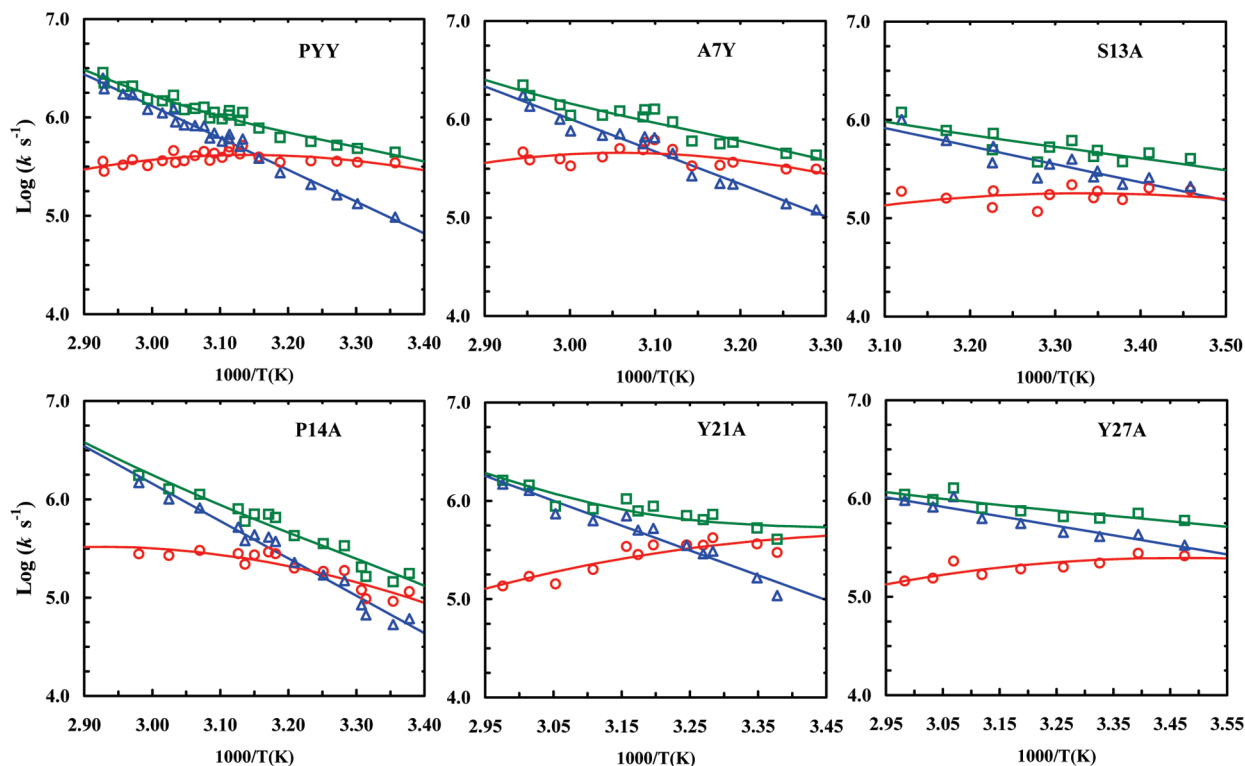


FIGURE 5: Arrhenius plots of the observed relaxation rates ( $\square$ ) as well as folding (O) and unfolding ( $\Delta$ ) rate constants for the peptides as indicated in the respective panels. For each peptide, lines represent global fits of the folding and unfolding rate constants to the Eyring equation [ $\ln(k) = \ln(D) - \Delta G^\ddagger/(RT)$ , where  $D$  is a constant and  $\Delta G^\ddagger$  is the free energy of activation]. In this work,  $D$  was arbitrarily set to  $10^{10} \text{ s}^{-1}$  and  $\Delta G_r^\ddagger$  and  $\Delta G_u^\ddagger$  were constrained so that  $\Delta G_r^\ddagger(T) - \Delta G_u^\ddagger(T) = \Delta G^\circ(T)$ , where  $\Delta G^\circ(T)$  is the equilibrium free energy of unfolding at temperature  $T$ .

Table 2: Folding and Unfolding Rate Constants of PYY and Its Mutants at 30 °C

| peptide | $k_f^{-1}$ ( $\mu\text{s}$ ) | $k_u^{-1}$ ( $\mu\text{s}$ ) |
|---------|------------------------------|------------------------------|
| PYY     | $2.8 \pm 0.5$                | $7.1 \pm 1.3$                |
| A7Y     | $3.6 \pm 0.6$                | $9.6 \pm 1.7$                |
| S13A    | $5.6 \pm 1.0$                | $2.8 \pm 0.5$                |
| P14A    | $6.9 \pm 1.2$                | $9.5 \pm 1.7$                |
| Y21A    | $2.8 \pm 0.5$                | $4.2 \pm 0.8$                |
| Y27A    | $4.3 \pm 0.8$                | $2.1 \pm 0.4$                |

example, if a mutation preferentially destabilizes the folding transition state and the folded state, the folding rate of the mutant is expected to be slower than that of the wild type, whereas the unfolding rate is largely unaffected. Thus, measurements of the folding kinetics of the mutant yield additional information that can be used to assess the characteristic of the transition state (15). As shown (Figure 5), both mutations in the turn region perturb the relaxation rate of PYY, consistent with the equilibrium CD results. A mutation of the turn sequence may increase the chain entropy of the peptide and/or remove a native side chain–side chain or side chain–backbone interaction. Thus, if the turn structure is formed (or becomes nativelike) in the folding transition state, such a mutation would destabilize not only the native state but also the transition state, resulting in a decrease in the folding rate. As indicated (Table 2), at 30 °C the folding time of P14A is increased by  $\sim 146\%$  from that of the wild type, whereas the unfolding time is only increased by  $\sim 34\%$ , suggesting that the transition state ensemble contains a nativelike turn, which in the case of PYY, is stabilized by the conformational constraint on the backbone  $\phi$  dihedral angle of Pro14. Further evidence supporting this notion comes from the folding time of S13A (Table 2), which

also shows an appreciable increase from that of the wild type (i.e., from 2.8 to 5.6  $\mu\text{s}$ ). In addition, the results obtained with S13A and P14A are consistent with the fact that the sequence of SPE is frequently found at the N-terminal end of  $\alpha$ -helices in proteins as it is an efficient end-capping group and can increase the rate of  $\alpha$ -helix formation (26). Furthermore, because the side chain of Ser13 can form two hydrogen bonds with the main chain nitrogen and the side chain of Glu16 (11), it is expected that elimination of these hydrogen bonds via mutation would result in not only a decrease in the folding rate but also an increase in the unfolding rate if only one of these hydrogen bonds is formed in the transition state, as observed (Table 2).

*Effect of the Hydrophobic Cluster on the Folding Thermodynamics and Kinetics of PYY.* It is well-known that the formation of a tightly packed hydrophobic cluster involving residues from both helices is essential to stabilization of the folded hairpin structure (3–5, 22). However, kinetically this can be achieved by either increasing the folding rate or decreasing the unfolding rate. To dissect these possibilities, we studied the thermodynamic and kinetic effects of two mutations (i.e., Y21A and Y27A) that weaken the hydrophobic interactions between the two helices (11). As expected, both mutations destabilize the PP fold (Figure 3 and Table 1), although the Y27A mutation has a much larger effect than the Y21A mutation, which is in agreement with the NMR measurements of Zerbe and co-workers (11).

As shown (Figure 5), mutation of either Y21 or Y27 to Ala results in a change in the  $T$ -jump-induced relaxation time of the peptide. It is clear that at 30 °C this change mostly arises from a change in the unfolding time (Table 2). For example, the unfolding time of Y27A is 2.1  $\mu\text{s}$ , which is significantly shorter than that (7.1  $\mu\text{s}$ ) of the wild type, whereas its folding time only shows a marginal increase in comparison to that of the wild type

Table 3: Folding and Unfolding Rate Constants of PYY and Its Mutants at 50 °C

| peptide | $k_f^{-1}$ ( $\mu$ s) | $k_u^{-1}$ ( $\mu$ s) |
|---------|-----------------------|-----------------------|
| PYY     | 2.4 ± 0.4             | 1.6 ± 0.3             |
| A7Y     | 2.2 ± 0.4             | 2.0 ± 0.4             |
| S13A    | 7.5 ± 1.4             | 1.2 ± 0.2             |
| P14A    | 3.6 ± 0.6             | 1.6 ± 0.3             |
| Y21A    | 4.6 ± 0.8             | 1.3 ± 0.3             |
| Y27A    | 5.5 ± 1.0             | 1.3 ± 0.2             |

(i.e., from 2.8 to 4.3  $\mu$ s). Thus, taken together, the results obtained with Y21A and Y27A suggest that the native hydrophobic cluster in PYY is formed at the downhill side of the folding free energy barrier.

**Effect of Temperature.** The kinetic data obtained at 30 °C support a folding mechanism in which the turn, but not the hydrophobic cluster, is formed in the transition state ensemble of PYY. To check whether such a conclusion remains true at higher temperatures, we further analyzed the folding and unfolding times of these PYY peptides at 50 °C. As shown (Table 3), the results for S13A and P14A corroborate the folding mechanism described above. However, those of Y21A and Y27A seem to indicate that the hydrophobic cluster is partially formed in the transition state, as their folding times are significantly longer than that of the wild type. In other words, the kinetic data obtained at 50 °C suggest a folding mechanism of PYY that is different from that deduced from the 30 °C data. While it is possible that the characteristics of the transition state ensemble of PYY show such a dependence on temperature, another possibility is that this apparent discrepancy arises from mutation-induced changes in the unfolded state. Many studies have shown that native and/or non-native hydrophobic contacts can exist in the denatured state of proteins (27–34). If such contacts exist in the thermally denatured state of wild-type PYY, they are expected to have a strong effect on the folding rate of the peptide. The NMR structure of PYY shows that Y21 and Y27 lie on the  $\alpha$ -helix side, while their side chains extend toward the PPII helix (Figure 1). Thus, it is possible that even in the unfolded state of PYY, interactions involving Y21 and Y27 and/or multiple residues on the PPII helix side persist. It is expected that such cross-strand interactions will reduce the entropic cost associated with formation of the turn by effectively restricting the conformational space of the unfolded polypeptide chain, thus accelerating folding. In other words, mutations that eliminate or decrease such cross-strand interactions are expected to decrease the folding rate, as observed.

In addition, we investigated the folding kinetics of the A7Y mutant, which was previously shown to be more stable than the wild-type peptide (11). Our CD results confirm that the A7Y mutation increases the thermal stability of the PP fold (Figure 3 and Table 1). However, the stability increase is marginal, and as a result, the changes in the folding and unfolding rates induced by this mutation are close to the uncertainty of the experiments (Tables 2 and 3). To avoid overinterpretation of the experimental results, no further assessment is made.

## CONCLUSIONS

In summary, we present a detailed mechanistic study of the folding mechanism of a naturally occurring helical hairpin (porcine PYY) that is free of disulfide bonds and other types of

cross-links. At a relatively low temperature (e.g., 30 °C), the effect of mutations in both the turn and hydrophobic cluster on the folding and unfolding rates of PYY supports a folding mechanism in which the turn is formed in the transition state, whereas the hydrophobic cluster is consolidated on the downhill side of the folding free energy barrier. However, a more complex picture emerges at relatively higher temperatures (e.g., 50 °C) at which the folding rate of PYY is more significantly affected, even by mutations that weaken the cross-helix interactions. While this result could manifest a temperature-dependent transition state ensemble, a more likely scenario is that it reflects changes in the unfolded conformational ensemble induced by such mutations. As the strength of the hydrophobic interaction increases with an increase in temperature, it is conceivable that the unfolded state ensemble of PYY is more compact at 50 °C than at 30 °C because of residual hydrophobic interactions between the two strands. Therefore, the comparatively slower folding rates of the hydrophobic deletion mutations at higher temperatures are reflections of their more flexible unfolded state ensembles, which allow the turn sequence to explore a larger region in the allowed conformational space, thus increasing the entropic penalty associated with turn formation and hence the folding time of the helical hairpin.

## REFERENCES

- Huffman, J. L., and Brennan, R. G. (2002) Prokaryotic transcription regulators: More than just the helix-turn-helix motif. *Curr. Opin. Struct. Biol.* 12, 98–106.
- Aravind, L., Anantharaman, V., Balaji, S., Babu, M. M., and Iyer, L. M. (2005) The many faces of the helix-turn-helix domain: Transcription regulation and beyond. *FEMS Microbiol. Rev.* 29, 231–262.
- Starovasnik, M. A., Braisted, A. C., and Wells, J. A. (1997) Structural mimicry of a native protein by a minimized binding domain. *Proc. Natl. Acad. Sci. U.S.A.* 94, 10080–10085.
- Zondlo, N. J., and Schepartz, A. (1999) Highly specific DNA recognition by a designed miniature protein. *J. Am. Chem. Soc.* 121, 6938–6939.
- Hodges, A. M., and Schepartz, A. (2007) Engineering a monomeric miniature protein. *J. Am. Chem. Soc.* 129, 11024–11025.
- Wetlaufer, D. B. (1973) Nucleation, rapid folding, and globular intrachain regions in proteins. *Proc. Natl. Acad. Sci. U.S.A.* 70, 697–701.
- Kim, P. S., and Baldwin, R. L. (1982) Specific intermediates in the folding reactions of small proteins and the mechanism of protein folding. *Annu. Rev. Biochem.* 51, 459–489.
- Fersht, A. R. (1997) Nucleation mechanisms in protein folding. *Curr. Opin. Struct. Biol.* 7, 3–9.
- Religa, T. L., Johnson, C. M., Vu, D. M., Brewer, S. H., Dyer, R. B., and Fersht, A. R. (2007) The helix-turn-helix motif as an ultrafast independently folding domain: The pathway of folding of Engrailed homeodomain. *Proc. Natl. Acad. Sci. U.S.A.* 104, 9272–9277.
- Woll, M. G., and Gellman, S. H. (2004) Backbone thioester exchange: A new approach to evaluating higher order structural stability in polypeptides. *J. Am. Chem. Soc.* 126, 11172–11174.
- Neumoin, A., Mares, J., Lerch-Bader, M., Bader, R., and Zerbe, O. (2007) Probing the formation of stable tertiary structure in a model miniprotein at atomic resolution: Determinants of stability of a helical hairpin. *J. Am. Chem. Soc.* 129, 8811–8817.
- Amunson, K. E., Ackels, L., and Kubelka, J. (2008) Site-specific unfolding thermodynamics of a helix-turn-helix protein. *J. Am. Chem. Soc.* 130, 8146–8147.
- Du, D., and Gai, F. (2006) Understanding the folding mechanism of an  $\alpha$ -helical hairpin. *Biochemistry* 45, 13131–13139.
- Dyer, R. B., Gai, F., Woodruff, W. H., Gilmanshin, R., and Callender, R. H. (1998) Infrared studies of fast events in protein folding. *Acc. Chem. Res.* 31, 709–716.
- Fersht, A. R., Matouschek, A., and Serrano, L. (1992) The folding of an enzyme. I. Theory of protein engineering analysis of stability and pathway of protein folding. *J. Mol. Biol.* 224, 771–782.
- Keire, D. A., Kobayashi, M., Solomon, T. E., and Reeve, J. R., Jr. (2000) Solution structure of monomeric peptide YY supports the functional significance of the PP-fold. *Biochemistry* 39, 9935–9942.

17. Lerch, M., Mayrhofer, M., and Zerbe, O. (2004) Structural similarities of micelle-bound peptide YY (PYY) and neuropeptide Y (NPY) are related to their affinity profiles at the Y receptors. *J. Mol. Biol.* *339*, 1153–1168.
18. Du, D., Zhu, Y., Huang, C.-Y., and Gai, F. (2004) Understanding the key factors that control the rate of  $\beta$ -hairpin folding. *Proc. Natl. Acad. Sci. U.S.A.* *101*, 15915–15920.
19. Du, D., Tucker, M. J., and Gai, F. (2006) Understanding the mechanism of  $\beta$ -hairpin folding via  $\phi$ -value analysis. *Biochemistry* *45*, 2668–2678.
20. Zhu, Y., Fu, X., Wang, T., Tamura, A., Takada, S., Saven, J. G., and Gai, F. (2004) Guiding the search for a protein's maximum rate of folding. *Chem. Phys.* *307*, 99–109.
21. Huang, C.-Y., Getahun, Z., Zhu, Y., Klemke, J. W., DeGrado, W. F., and Gai, F. (2002) Helix formation via conformational diffusion search. *Proc. Natl. Acad. Sci. U.S.A.* *99*, 2788–2793.
22. Fezoui, Y., Weaver, D. L., and Osterhout, J. J. (1994) De novo design and structural characterization of an  $\alpha$ -helical hairpin peptide: A model system for the study of protein folding intermediates. *Proc. Natl. Acad. Sci. U.S.A.* *91*, 3675–3679.
23. Williams, S., Causgrove, T. P., Gilmanshin, R., Fang, K. S., Callender, R. H., Woodruff, W. H., and Dyer, R. B. (1996) Fast events in protein folding: Helix melting and formation in a small peptide. *Biochemistry* *35*, 691–697.
24. Walsh, S. T. R., Cheng, R. P., Wright, W. W., Alonso, D. O. V., Daggett, V., Vanderkooi, J. M., and DeGrado, W. F. (2003) The hydration of amides in helices: A comprehensive picture from molecular dynamics, IR, and NMR. *Protein Sci.* *12*, 520–531.
25. Mukherjee, S., Chowdhury, P., and Gai, F. (2007) Infrared study of the effect of hydration on the amide I band and aggregation properties of helical peptides. *J. Phys. Chem. B* *111*, 4596–4602.
26. Wang, T., Zhu, Y., Getahun, Z., Du, D., Huang, C.-Y., DeGrado, W. F., and Gai, F. (2004) Length-dependent helix-coil transition kinetics of nine alanine-based peptides. *J. Phys. Chem. B* *108*, 15301–15310.
27. Neri, D., Billeter, M., Wider, G., and Wüthrich, K. (1992) NMR determination of residual structure in a urea-denatured protein, the 434-repressor. *Science* *257*, 1559–1563.
28. Wilson, G., Hecht, L., and Barron, L. D. (1996) Residual structure in unfolded proteins revealed by Raman optical activity. *Biochemistry* *35*, 12518–12525.
29. Mok, Y.-K., Kay, C. M., Kay, L. E., and Forman-Kay, J. (1999) NOE data demonstrating a compact unfolded state for an SH3 domain under non-denaturing conditions. *J. Mol. Biol.* *289*, 619–638.
30. Tang, Y., Rigotti, D. J., Fairman, R., and Raleigh, D. P. (2004) Peptide models provide evidence for significant structure in the denatured state of a rapidly folding protein: The villin headpiece subdomain. *Biochemistry* *43*, 3264–3272.
31. Tucker, M. J., Oyola, R., and Gai, F. (2005) Conformational distribution of a 14-residue peptide in solution: A fluorescence resonance energy transfer study. *J. Phys. Chem. B* *109*, 4788–4795.
32. Mok, K. H., Kuhn, L. T., Goetz, M., Day, I. J., Lin, J. C., Andersen, N. H., and Hore, P. J. (2007) A pre-existing hydrophobic collapse in the unfolded state of an ultrafast folding protein. *Nature* *447*, 106–110.
33. Zhou, R., Eleftheriou, M., Royyuru, A. K., and Berne, B. J. (2007) Destruction of long-range interactions by a single mutation in lysozyme. *Proc. Natl. Acad. Sci. U.S.A.* *104*, 5824–5829.
34. Das, P., King, J. A., and Zhou, R. (2010)  $\beta$ -Strand interactions at the domain interface critical for the stability of human lens  $\gamma$ -crystallin. *Protein Sci.* *19*, 131–140.